Geochemistry Geophysics Geosystems G3

Article
Volume 11, Number 6
22 June 2010
Q06010, doi:10.1029/2009GC003014
ISSN: 1525-2027

Published by AGU and the Geochemical Society

Structure and evolution of the intracratonic Congo Basin

A. G. Crosby
Bullard Laboratories, Department of Earth Sciences, University of Cambridge, Cambridge CB3 0EZ, UK (alistair.crosby@uk.bp.com)

S. Fishwick
Department of Geology, University of Leicester, Leicester LE1 7RG, UK (sf130@leicester.ac.uk)

N. White
Bullard Laboratories, Department of Earth Sciences, University of Cambridge, Cambridge CB3 0EZ, UK (njw10@cam.ac.uk)

[1] Surface wave tomography, heat flow, and crustal thickness measurements have demonstrated that the thickness of the continental lithosphere varies by at least a factor of 2. Since the thermal time constant of the lithosphere depends upon the square of its thickness, subsidence records of extensional sedimentary basins offer a potential way of extending these observations into the past. Here we examine the Congo basin, a large and iconic intracratonic sedimentary basin in Central Africa. This roughly circular basin covers an area in excess of 1.4×10^6 km^2 with more than 5 km thickness of sedimentary rocks, the oldest parts of which are late Precambrian in age. First, we assess the thickness of the lithosphere. We have estimated its thickness across Africa using maps of shear wave velocity obtained by inversion of fundamental and higher-mode surface waveforms. The Congo Basin sits on 220 ± 30 km thick lithosphere and appears to be part of a southern core to the continent encompassing both Archean cratons and Proterozoic mobile belts. This thickness is consistent with published estimates from kimberlites. Reappraisal of legacy seismic reflection images demonstrates that the sedimentary section is underlain by a Late Precambrian rift zone and that the basin is still subsiding today. Subsidence modeling of two deep wells is consistent with uniform extension and cooling of the lithosphere by a factor of 1.2 during latest Precambrian and Cambrian time; we argue that the exceptional 0.55 Ga history of the basin is a direct consequence of the lithospheric thermal time constant being a factor of 4 longer than normal. Today, the basin coincides with a long-wavelength −30 to −40 mGal gravity anomaly. We interpret this gravity anomaly as the surficial manifestation of 400–600 m of recent mantle convective drawdown in response to the onset of upwelling plumes around the flanks of the southern African continent. The alternative explanation, that it is the static manifestation of locally thick lithosphere, is inconsistent with global trends of mantle density depletion. Our interpretation is consistent with fast seismic velocities observed throughout the sublithospheric upper mantle underneath the basin and recent geodynamic modeling.

Components: 11,600 words, 14 figures.

Keywords: Congo Basin; lithosphere; intracratonic basins; tomography; gravity.

Index Terms: 8109 Tectonophysics: Continental tectonics: extensional (0905); 8103 Tectonophysics: Continental cratons (1236); 7218 Seismology: Lithosphere (1236).

Received 22 December 2009; **Revised** 1 April 2010; **Accepted** 7 April 2010; **Published** 22 June 2010.

Crosby, A. G., S. Fishwick, and N. White (2010), Structure and evolution of the intracratonic Congo Basin, *Geochem. Geophys. Geosyst.*, *11*, Q06010, doi:10.1029/2009GC003014.

1. Introduction

[2] The existence of sedimentary basins over regions of thick lithosphere has long posed a problem. How and why did these basins form? Do they differ in their evolution from better known basins over lithosphere of normal thickness? We now know that many, but not all, basins are formed by extension of the crust and lithospheric mantle. Extension causes basement normal faulting and rapid synrift subsidence, followed by more gradual postrift subsidence as the elevated hot mantle underneath cools [*McKenzie*, 1978]. Since the time constant of cooling varies as the square of the lithospheric thickness, basins over thick lithosphere should accumulate sediments for three or four times as long as those over thin lithosphere. Understanding whether these predictions are correct, and whether lithospheric thickness exerts other controls on basin architecture, provides important constraints on the structure and geodynamic stability of the continental lithosphere. Unfortunately, such studies have been hampered in the past by a lack of understanding of how lithospheric thickness varies with location.

[3] A crucial advance has come from seismic tomographic inversions of large inventories of earthquake records. Physical properties of the upper mantle have been estimated from the seismic models using mineral physics data to estimate temperatures [e.g., *Goes et al.*, 2000; *Godey et al.*, 2004], or through an empirical relationship linking velocity and temperature based on oceanic cooling models to directly map the thickness of the lithosphere [*Priestley and McKenzie*, 2006]. These maps confirm that many sedimentary basins are found close to the rifted margins of the continents where the lithosphere does not differ significantly in thickness from the surrounding oceans. However, other basins (e.g., the Michigan and Hudson Bay Basins) occur within regions where the lithosphere is a factor of 2 thicker. These basins contain several kilometers of sediment and are underlain by normal faults, and appear to be at least partly extensional in origin [e.g., *Hanne et al.*, 2004].

[4] The origin of these intracratonic basins has long been controversial. There is no consensus on the origin of their often circular shapes, on whether they are primarily extensional and, if so, on the extent to which their subsidence can be explained using simple one-dimensional plate models [e.g., *McKenzie*, 1978; *Sleep and Sloss*, 1978; *Kaminski and Jaupart*, 2000; *Kominz et al.*, 2001; *Armitage and Allen*, 2010]. These arguments have not been helped by the general absence of good quality seismic reflection data that could image extensional faulting. An important problem is that the fixed temperature basal boundary condition in plate models may be too simple. Thick, chemically depleted lithosphere does not automatically rethicken after extension, and the process of small-scale convection that ultimately maintains the thickness of the plates is time-dependent and varies with the initial thermal anomaly. *Sleep* [2009], for instance, has recently explained observations of subsidence in the Michigan Basin in terms of small-scale convection of ponded plume material under a thinned lithospheric lid. However, it is unclear how applicable these particular starting conditions are to all intracratonic basins. Moreover, the subsidence of the cooling oceanic lithosphere and of sedimentary basins over thin lithosphere such as the North Sea has been well explained to first order using simple plate cooling models, even though many of the same boundary condition concerns apply [e.g., *Newman and White*, 1999; *Crosby et al.*, 2006].

[5] Of all the intracratonic basins, the Congo basin illustrated in Figures 1–6 is the most striking. This basin, also referred to as the Cuvette Centrale, forms a circular depression of approximately 1.4×10^6 km^2 that has accumulated 4–9 km of sediments from Late Precambrian time until the present day. It now coincides with both a region of ~200 km thick lithosphere and a pronounced long-wavelength negative gravity anomaly. *Daly et al.* [1991, 1992] described the available well log and seismic reflection data in detail and showed that its evolution began with lithospheric extension during Late Precambrian time. However, they could not explain why subsidence continued (albeit with significant interruptions) for more than 0.5 Ga until Cenozoic times, when other extensional basins such as the North Sea have a history that is almost three times shorter. *Hartley and Allen* [1994] argued that this later phase of subsidence could be explained as the surface response to a downwelling mantle plume, which would also explain the regional negative gravity anomaly. The recent geodynamic predictions of *Forte et al.* [2010] support this view, and the evolution of the Hudson Bay basin in Canada has been explained in a similar way [e.g., *Peltier et al.*, 1992; *Perry et al.*, 2003]. Other authors have sought to place a high-density anomaly within the mantle lithosphere [e.g., *Downey and Gurnis*, 2009].

[6] Given these differing interpretations, we believe that a reassessment of the structure and evolution

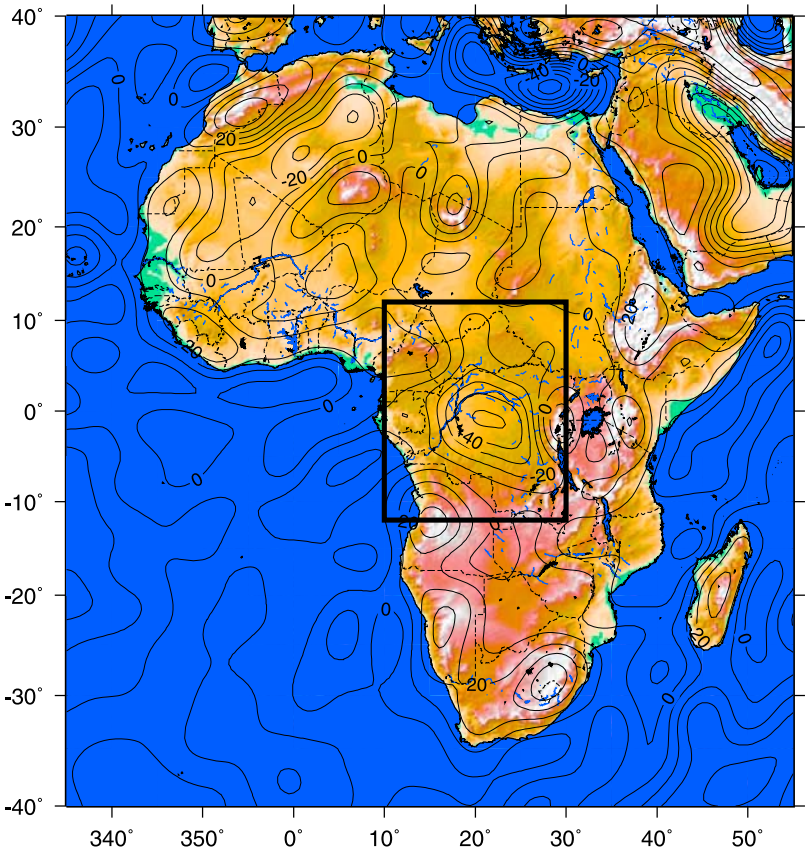

Figure 1. Regional map of Africa showing the area of interest in Figure 2. Contours are GRACE gravity anomalies filtered to spherical harmonic degree 110 (360 km wavelength); they illustrate the large negative anomaly under the basin surrounded by gravity highs and delineate the regional pattern of mantle convection.

of the Congo Basin is timely. In this study, we present three important and interconnected results: a revised map of African lithospheric thickness based on the inversion of surface waveforms, an analysis of the subsidence history of two deep wells, and a model for the pronounced long-wavelength gravity anomaly. Our results, together with a reappraisal of unpublished legacy seismic reflection data, are then used to build a simple and self-consistent large-scale model for this most enigmatic of basins, which may shed light on the development of other intracratonic basins, and on the evolution and structure of thick lithosphere in general.

2. Congo Basin

[7] Limited knowledge of the shallow subsurface structure of the Congo Basin is known from 2900 km of 2-D reflection seismic data acquired in twenty discontinuous segments between 1974 and 1976 by an industrial consortium of Shell, Texaco and Esso; by two deep (4.3–4.6 km) boreholes drilled by the same consortium in 1981; and by two older, shallower (2 km) wells drilled between 1952 and 1956. There is as yet no proven hydrocarbon potential, and for this reason further exploration has been limited. A synthesis of our current understanding is given by *Exploration Consultants Ltd.* (*ECL*) [1988], *Lawrence and Makazu* [1988], *Daly et al.* [1991, 1992], and *Giresse* [2005], and is summarized below and in Figures 2–5.

[8] The present-day basin comprises at least three NW/SE trending subbasins separated by ~100 km wide basement highs, later cut by NE/SW trending strike-slip faults. Mapped structure is shown in Figure 2d. Figure 2b shows that the basin forms one continuous depocenter: the maximum sediment thickness is ~9 km, with an average value of approximately 4 km in the deep basin. The two deep boreholes reached sediments of Vendian age, but did not penetrate basement rocks. Figure 3 shows a composite log from the deep Mbandaka-1 well, and Figure 4 shows two typical seismic reflection images.

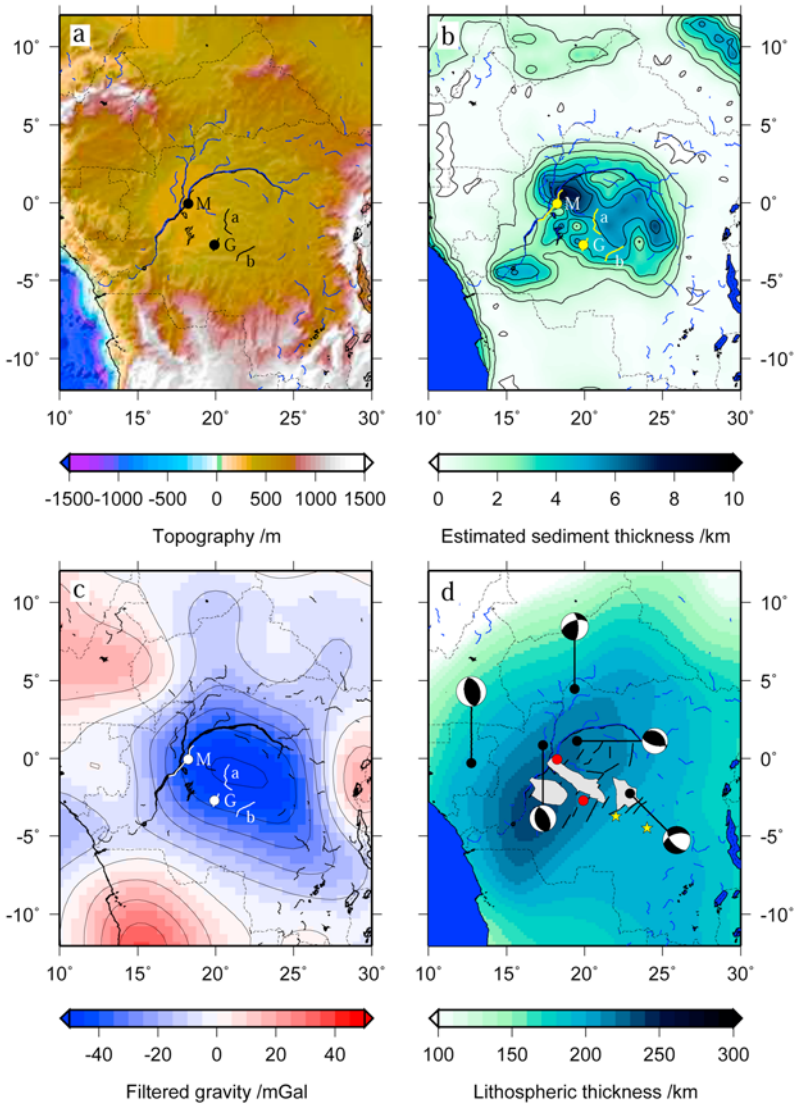

Figure 2. The Congo basin. (a) Topography. Locations of deep wells, Mbandaka-1 and Gilson-1, are indicated by M and G, respectively. Black lines are seismic sections illustrated in Figure 4. Basin coincides with a 0.5 km depression with respect to its surroundings. (b) Approximate sediment thickness from *Laske and Masters* [1997]. Contours every 1 km from 1 km. (c) GRACE gravity anomalies filtered to exclude wavelengths shorter than ~500–800 km. Contours are 10 mGal. Note the approximately −30 mGal anomaly over the whole width of the basin, rising to approximately −40 mGal in the center. (d) Lithospheric thickness from this study. Gray indicates structural elements mapped by *ECL* [1988] together with recent seismic focal mechanisms (m_w 5.13–5.66). Thin black lines indicate fault traces from *ECL* [1988]. Yellow stars show locations of kimberlites analyzed in the study of *Batumike et al.* [2009], who estimated the thickness of the lithosphere to be ~210 km.

Other composite seismic sections from *ECL* [1988] are illustrated in summary form in Figure 5. Extensional normal faults and tilted blocks are clearly visible in Early Paleozoic sediments, although there is also evidence in the form of reverse faults and gentle folding for subsequent mild crustal shortening in Late Cambrian and Permo-Triassic times. The tilted blocks are ~100 km in width, which is twice as wide as is observed in the East African rift system where the lithosphere is thinner. *Foster and Nimmo* [1996] suggested differences in fault block width result from lower thermal gradients and thus higher strength in the brittle lithosphere. Early synrift sedimentary rocks were deposited in a shallow water environment that rapidly deepened and there has been no magmatism. There is obvious erosional truncation of pre-Triassic (i.e., Upper Zaire Sequence) sedimentary rocks at the

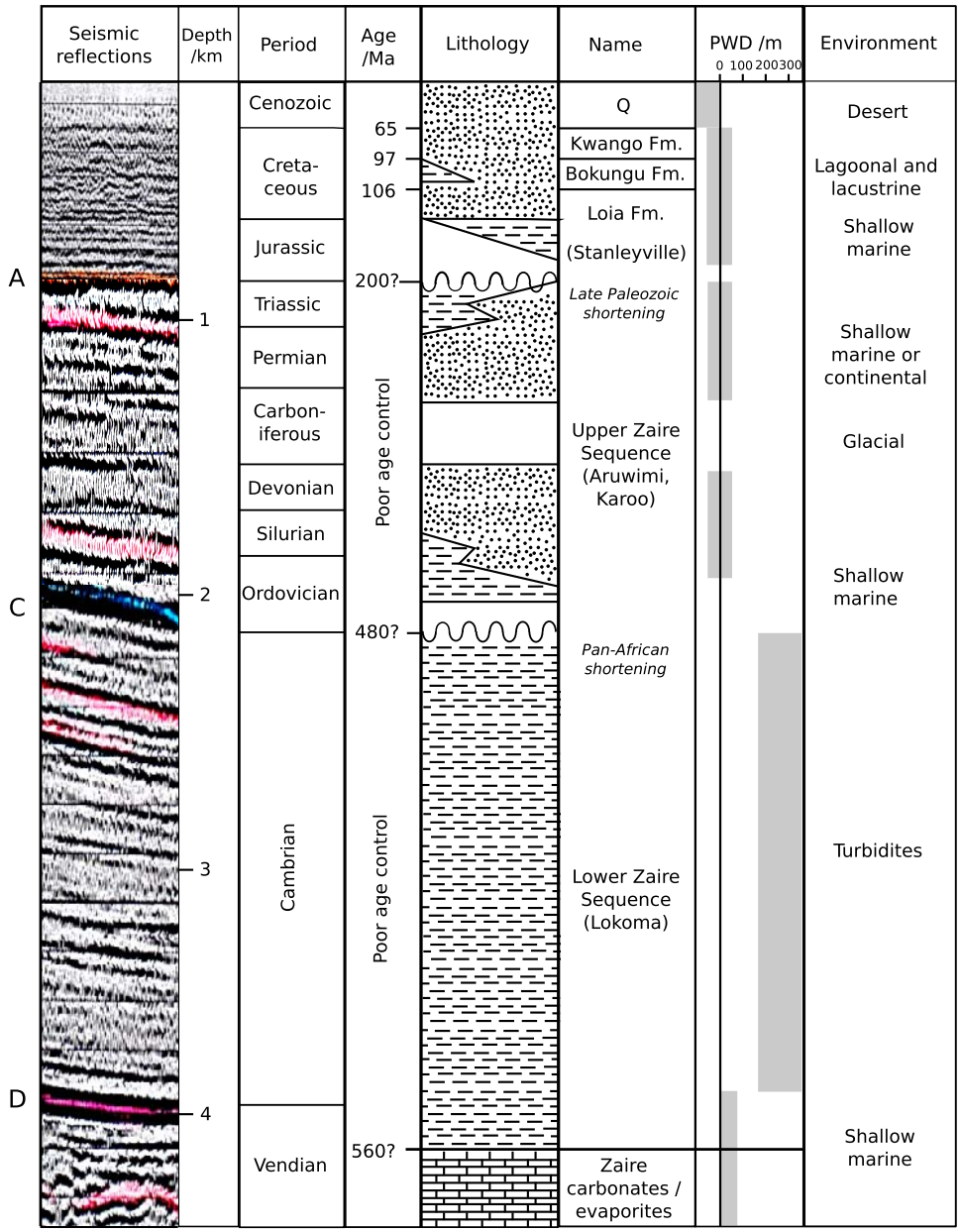

Figure 3. Stratigraphic section from the Mbandaka-1 deep well showing the principal units and variation in water depth. Data are from *ECL* [1988] and *Daly et al.* [1992]. Note that pre-Mesozoic ages are highly uncertain, and there is little control on the onset time of rifting since neither well penetrated basement rocks.

edge of the major basement blocks, especially the Kiri High, although both wells penetrate apparently intact stratigraphic sections. *Daly et al.* [1991] have interpreted this reactivation as a far-field response to events in the construction of Gondwana, by analogy with contemporary Central Asia. During the main Pan-African event at the end of Cambrian times, we speculate that most of the deformation was taken up in the surrounding mobile belts, with only minor adjustment of the thick, cold and therefore probably strong lithospheric core underlying the basin. However, we do not believe that the basin can be explained simply by foreland loading because the basin shallows, rather than deepens, toward its edge. The Mesozoic and Cenozoic (i.e., post-A; see Figure 3) sections postdate the periods of deformation and have only minor faulting.

[9] Within the basin, water depths have been shallow marine or lagoonal since Late Cambrian times, and Cenozoic sedimentary rocks are consistent with a fluvial and then aeolian environment.

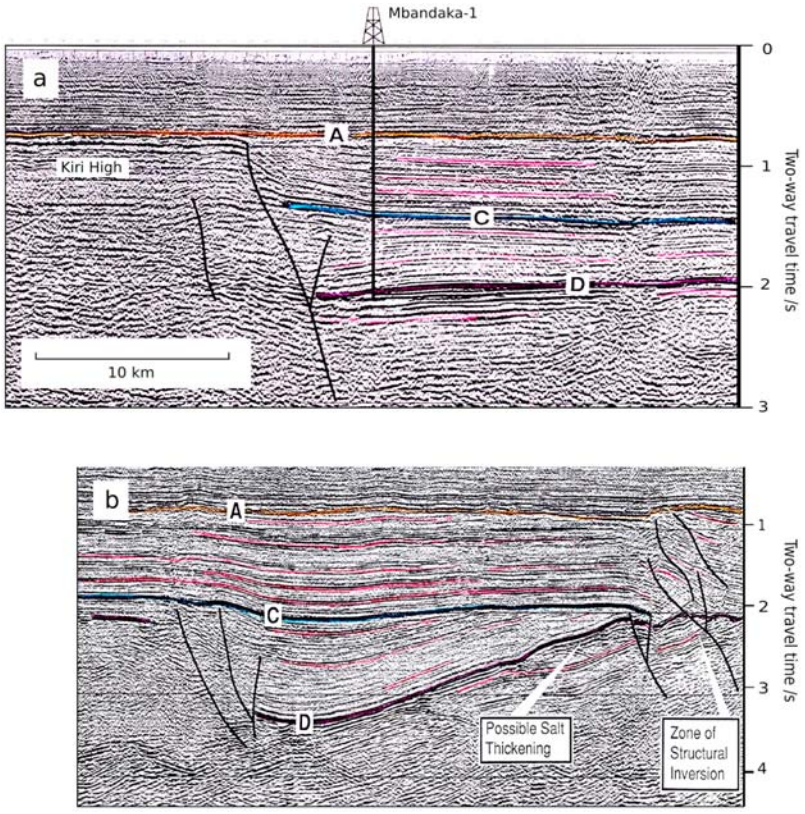

Figure 4. (a) Seismic reflection image in the vicinity of Mbandaka-1, reproduced from *ECL* [1988]. (b) Enlarged section of central portion of Figure 5a to the right of the Kiri High from same source. Note clear tilted fault block geometry and stratigraphic growth. Horizontal scale is the same in both Figures 4a and 4b.

Cenozoic uplift of the basin surroundings [e.g., *Nyblade and Robinson*, 1994, *Walford and White*, 2005; *Al Hajri et al.*, 2009] has accounted for the most recent phase of sediment input, with drainage concentrating in the Congo River, the second largest in the world by discharge. Figure 2d illustrates seismicity in the basin during the last 40 years as modeled by *Foster and Jackson* [1998], *Ayele* [2002], and J. Jackson (personal communication, 2009). The five magnitude 5–6 events illustrated have shallow (6–10 km) compressional mechanisms with minor strike-slip components suggesting mild surface shortening. One exception is event 811118, which shows extension, but this event is poorly constrained because the first motion waveforms lie close to the P nodal planes.

[10] Figures 1 and 2c show gravity anomalies in the vicinity of the basin. At the scale of the basin, the most striking feature is a large long-wavelength (~40 mGal) negative anomaly which coincides with the areal extent of the basin and extends ~400 km to the northwest and southeast. *Hartley and Allen* [1994] were the first to show that this anomaly, with a wavelength of ~2000 km, is too large to result from variations in crustal structure unless the elastic thickness of the lithosphere is ~100 km. Since this value is unlikely on rheological grounds [*McKenzie and Fairhead*, 1997], the gravity anomaly must instead result from density variations within the mantle.

3. Geophysical Context: Surface Wave Tomography and Lithospheric Structure

[11] While seismic reflection data gives direct constraints on the near surface structure beneath the Congo Basin, the scarcity of permanent seismic stations means that tomographic models presently provide most of the information on the seismic structure of the deep crust and lithospheric mantle. In the last decade, there have been a number of large-scale models of the lithospheric mantle beneath Africa produced using surface wave tomography [e.g., *Ritsema and van Heijst*, 2000; *Sebai et al.*, 2006; *Pasyanos and Nyblade*, 2007; *Priestley and McKenzie*, 2006]. An advantage of these surface wave studies is that because of the

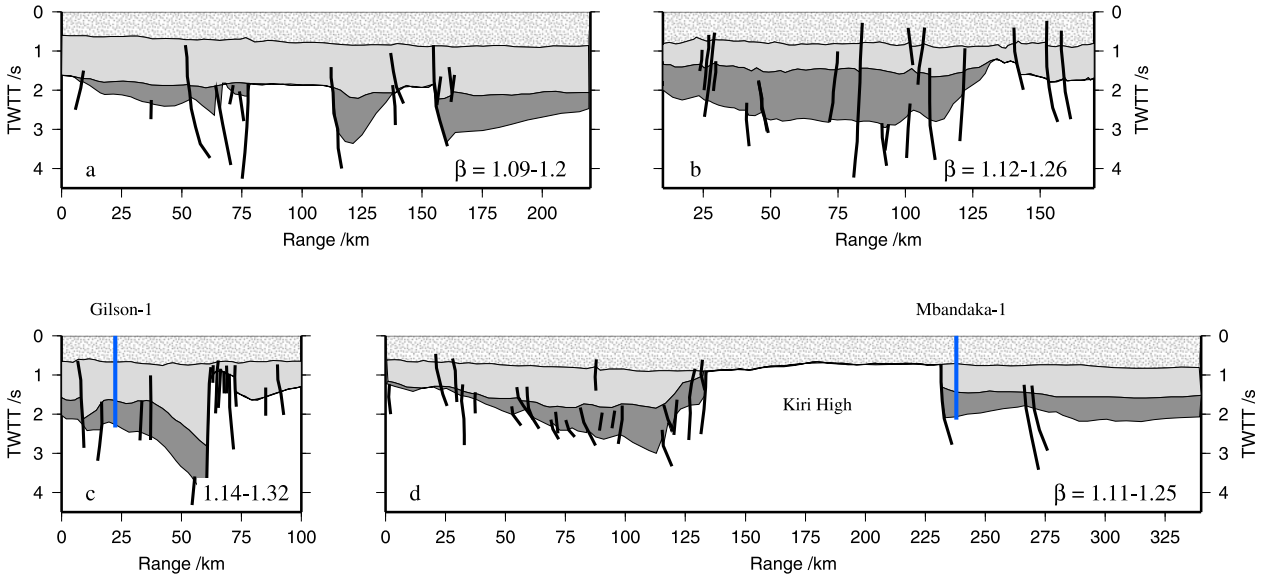

Figure 5. Summary structural cross sections along four segments illustrated in Figure 1, amended from *ECL* [1988]. Dark gray shading indicates Cambrian, white indicates Ordovician-Triassic, and stippled area indicates post-Triassic rocks. Locations of Mbandaka-1 and Gilson-1 wells are shown as thick blue lines and appear to penetrate relatively undisturbed stratigraphic sections. Note erosional truncation of the Upper Zaire Sequence against the Kiri High, showing mild post-Cambrian shortening. Estimates of β factors from summed horizontal displacements of mappable faults are annotated. Lower limit is observation, and upper limit is from double total extension estimate since most faults are seismically invisible [e.g., *Walsh et al.*, 1991]. Calculation included treating reactivated reverse faults as normal faults since we are concerned with initial extension. Note consistency with modeling in Figure 8.

horizontally propagating waves, even in areas with few stations, a good path coverage can be obtained due to the crossing paths of more distant station and event pairs. Body wave tomography for this region is best exploited using multibounce SH wave tomography [e.g., *Grand*, 2002; *Simmons et al.*, 2009]; the method yields an improved resolution in the upper mantle and permits direct comparison with the surface wave models. The recent work of *Begg et al.* [2009] focuses discussion on the African upper mantle and is therefore the best comparison with our present study. Beneath the Congo basin nearly all the models show a fast velocity anomaly, typically explained as a cold lithospheric root, which extends to depths of around 200–300 km. In contrast, the model of *Pasyanos and Nyblade* [2007] indicates fast velocity anomalies extending to these depths only on the western edge of the basin, with slower wave speeds observed beneath the center and east.

[12] In Figure 6a, we present summary results from a recent tomographic study of the continent [see also *Al Hajri et al.*, 2009]. The tomography is based on a two stage process similar to that used by *Priestley and McKenzie* [2006]. Initially, a slightly modified version of the waveform inversion code of *Debayle* [1999] is used to calculate the 1-D average model of the shear wave speed for the path between source and receiver. In order to improve the reliability of the data set, the waveform inversion is run from multiple starting models [*Fishwick et al.*, 2005], and only data with a consistent set of final models are accepted for the next stage. The increased path coverage and manual intervention is the crucial difference between our work and that of previous authors [e.g., *Priestley and McKenzie*, 2006]. The final set of such path average models is then combined within a tomographic inversion to derive a model of the regional velocity structure. Figure 7 shows the path coverage and ray path density for the tomographic inversion. Inclusion of data from the recent seismic experiment in Cameroon significantly improves the path coverage across the Congo Basin in comparison to the earlier studies [*Tibi et al.*, 2005]. A large number of ray paths (>10000), consistently high path density, and wide azimuthal variations in path direction gives good confidence in the potential resolution of the data set. Results from the tomography are in agreement with the majority of studies, highlighting fast velocities relative to the reference model ak135

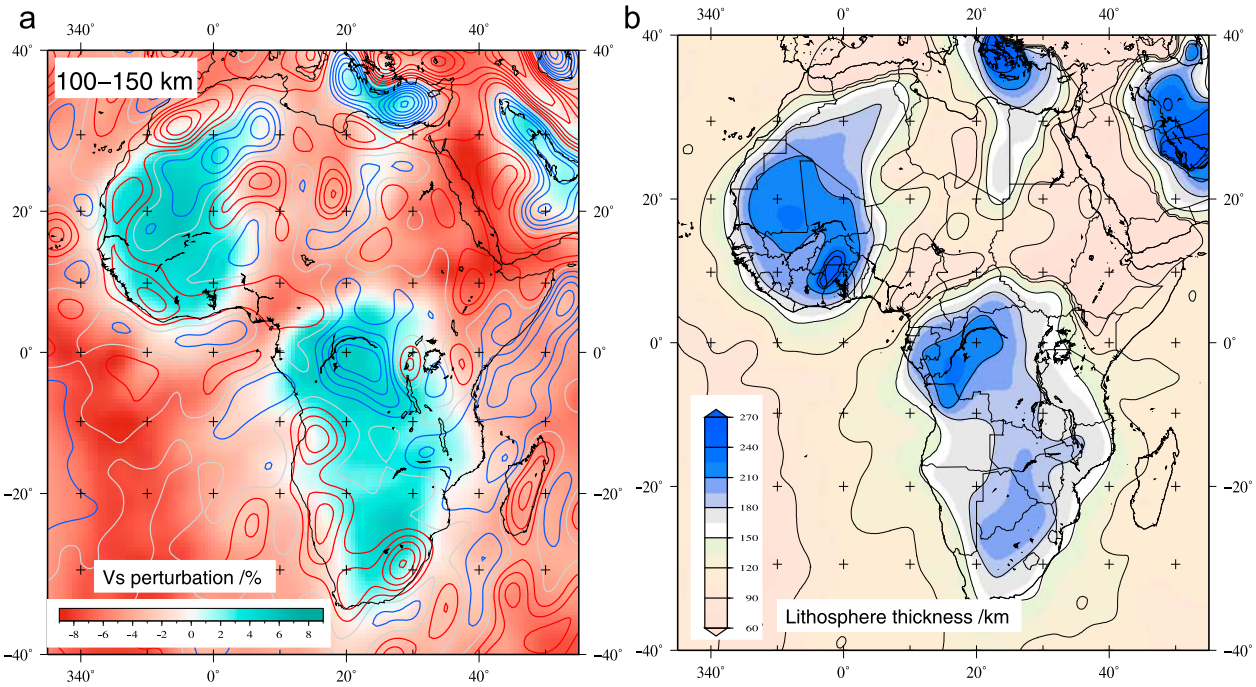

Figure 6. (a) Average shear wave velocity anomaly between depths of 100 and 150 km from the surface wave tomographic model of Fishwick [*Al Hajri et al.*, 2009], which clearly delineates major cratons. Contours are from GRACE gravity model filtered to exclude components shorter than 600 km [*Tapley et al.*, 2005]: note close correlation with velocity anomalies away from the main cratons. The Hoggar, Tibesti, Bie, Namibian, and South African domal swells are clearly visible and appear to result from upwelling mantle plumes. The Congo basin is associated with a substantial gravity low. (b) Estimate of lithospheric thickness using the method of *Priestley and McKenzie* [2006]. The Congo basin overlies thick lithosphere.

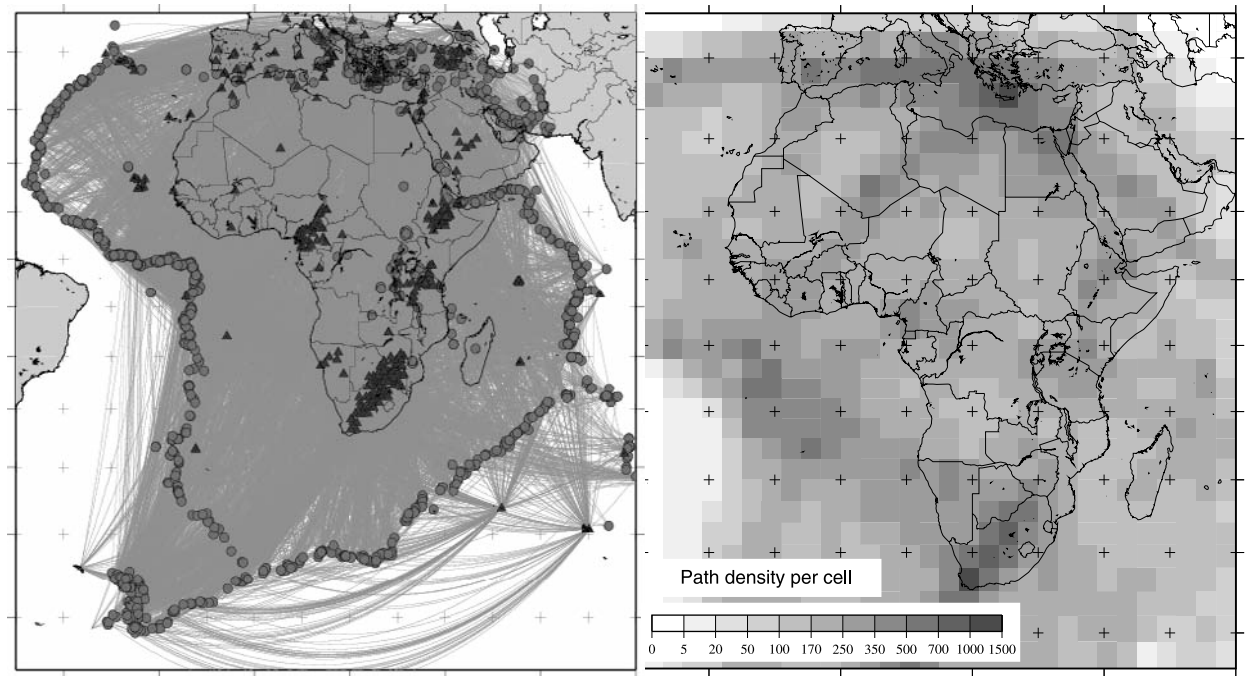

Figure 7. Ray coverage diagrams. Earthquakes are shown by dark gray circles, and stations are shown by solid black triangles. Note uniformly good path coverage, aided over the Congo Basin by data from the Cameroon Line experiment [*Tibi et al.*, 2005].

extending to a depth of at least 175 km beneath most of the Congo Basin.

[13] Although it is not the purpose of this paper to resolve discrepancies between the different models, some comment is required to justify our choice of this model for constructing the lithospheric template for later gravity and subsidence modeling. There are significant differences in methodology between the different models. For example, *Pasyanos and Nyblade* [2007] use group velocities, measured using frequency-time analysis, and model the lithospheric structure in terms of a uniform velocity lid for the uppermost mantle. One possibility is that the increasing uncertainty on the group velocity measurements at longer period may mean that the deeper structure is less well resolved. The tomographic results presented in this study and in much of the previous work use different styles of waveform modeling to constrain the path average structure, and do not require a uniform velocity lid within their parameterization of the velocity variations [e.g., *Sebai et al.*, 2006; *Priestley and McKenzie*, 2006; *Begg et al.*, 2009]. The vertical parameterization may have important consequences for the velocities observed in different models. Using a two station method, *Lebedev et al.* [2009] suggest that there is a strong velocity gradient (from slower to faster velocities) beneath the northwest edge of the Congo Craton. If this style of gradient exists beneath the center of the basin it will be very hard to resolve the true structure using a "lid" representation of the velocities. Further investigations combining the different seismic data sets should improve our understanding of the present discrepancies.

[14] In order to estimate a lithospheric thickness, we apply the method of *Priestley and McKenzie* [2006]. They combined thermal models of the Pacific Ocean and pressure-temperature estimates from kimberlites with tomographic models of shear velocity in order to find an empirical relationship between velocity, temperature and pressure. Using their parameterization, it is possible to convert absolute shear wave velocities from a tomographic model into estimates of temperature. The lithospheric thickness is then constructed by calculating the depth at which the temperature profile reaches the isentrope for a potential temperature of 1315°C. Our results are shown in Figure 6b. One of the main limitations of this method is that in continental regions the temperature estimates at shallow mantle depths (50–125 km) are less reliable. These errors may be due smearing of low crustal velocities due to the limited vertical resolution of the surface wave tomography [*Priestley and McKenzie*, 2006], or may be related to observations suggesting that within many regions of thick lithosphere the seismic velocity distribution cannot be explained by one single composition and a cratonic geotherm [*Fishwick and Reading*, 2008; *Pedersen et al.*, 2009; *Lebedev et al.*, 2009]. However, when lithospheric thicknesses exceed 150 km, *Priestley and McKenzie* [2006] suggest that the vertical uncertainty in their measurements of total lithospheric thickness is approximately ±20 km.

[15] Figure 6b shows clearly the long-observed variations in lithospheric structure between the cratonic regions and the surrounding mobile belts, rift zones and oceans. Beneath cratonic regions, there are also significant differences in thickness. The thickest lithosphere is evident beneath parts of the West African Craton. In contrast, the model shows much thinner lithosphere beneath the Tanzanian Craton, within the East African Rift zone. This estimate of around 160 km is significantly different to the model of *Priestley and McKenzie* [2006], who estimate thicknesses in excess of 250 km, but is consistent with results from a detailed array analysis of surface waves from a temporary deployment in the area [*Weeraratne et al.*, 2003]. Receiver function studies also documented a deflection of the 410 km phase discontinuity and infer the existence of a plume responsible for the elevated topography [*Huerta et al.*, 2009]. Beneath the Congo Craton the thickness varies from 240 km in the western margin to around 180 km toward the east. It is therefore reasonable to use a lithospheric template with a thickness of 200 km for the subsidence and gravity modeling in sections 4 and 5. Importantly, these estimates are also in excellent agreement with the work of *Batumike et al.* [2009], who used geochemical analysis of garnet xenocrysts from kimberlites in the Mbuji Mayi and Luebo areas of the southern D. R. Congo to estimate a lithospheric thickness of 205 ± 5 km (Figure 2d).

[16] All other factors being equal, at a given depth a region of thick mantle lithosphere will be cooler and more dense than adjacent lithosphere of standard thickness. However, evidence from kimberlite nodules suggests that thickened lithosphere is also depleted in garnet as a result of prior melt extraction, which causes a chemical reduction in density. The isopycnal hypothesis, first articulated by *Jordan* [1978], states that this reduction in density due to melt extraction balances the gain in density due to cooling, thereby stabilizing regions of thick lithosphere against convective instability. This conclusion has been supported in general terms by

more recent geodynamic inversions although the balance is unlikely to be exact [e.g., *Forte and Perry*, 2000; *Simmons et al.*, 2009]. Rare Earth Element modeling of kimberlites implies that the depleted source is approximately 20–70 kg m^{-3} lighter than the equivalent MORB source [e.g., *Tainton and McKenzie*, 1994]. In Appendix A, we use a global database of crustal thickness measurements to make our own expected estimates based on isostasy, and find them to be roughly in agreement (mean depletion 33 ± 16 kg m^{-3} for $L > 150$ km).

4. Subsidence Modeling

[17] The observation that the oldest basin sedimentary rocks are tilted by normal faulting implies that at least some of the growth in accommodation space results from extension of the continental crust. In this section, we analyze borehole subsidence records from the two deep wells to assess the extent to which lithospheric, as opposed to just crustal, extension can account for the sustained growth of the basin over time. *Daly et al.* [1992] implied that the Mesozoic phase of basin growth could not be explained as postrift subsidence following Early Cambrian extension because the time scales are too long. However, this analysis is only valid for lithosphere of normal thickness. The lithosphere under the Congo Basin is anomalously thick today and, since the duration of postrift subsidence varies as its square, we would have expected the basin to grow throughout Phanerozoic time. More specifically, 560 Ma represents 10 thermal time constants if the lithosphere is 120 km thick, but only 3.5 time constants if the lithosphere is 200 km thick. We assume here that the lithosphere achieved its present thickness by Vendian times, although our data do not discount small subsequent increases in thickness due to shortening.

[18] We have calculated the tectonic subsidence history of the two deep wells (Figure 8; see *Sclater and Christie* [1980] and *White* [1994] for details). This analysis requires knowledge of both the age of the sedimentary rocks and the paleowater depths at the time of deposition (Figure 3). We are aware that age constraints are limited prior to Mesozoic time (isolated Cambrian acritarchs and Carboniferous miospores), and since neither well reached basement, the exact timing of initial rifting is uncertain. For this reason, we have included no data between Cambro-Orodovician (best estimate top synrift) and Mesozoic times in our backstripping. Nevertheless, it can be seen that although there is clearly local variation in the growth of accommodation space during extension, the Mesozoic subsidence gradients of both wells can be well explained by lithospheric thermal decay after Cambrian extension of a thick (~200 km) lithospheric template by a factor of ~1.2. This extension factor is consistent with estimates made from summation of the horizontal displacements across mappable normal faults in Figure 5. In places, normal faults have clearly been structurally inverted, but the original extensional displacement can still be estimated. Figure 8 shows that the synrift subsidence is ~200 m greater than predicted by the model which best fits the Mesozoic section. Possible explanations are loss of sediment due to uplift and erosion, which is not unexpected since *Daly et al.* [1992] document at least two depositional hiatuses corresponding to episodes of regional tectonism; and selective drilling in the deepest part of fault blocks (Figure 5).

[19] Details of our updated stretching model appropriate for thick and depleted lithosphere are given in Appendix C. To fit the same observations, a standard 120 km template would require continued extension into Cenozoic times, which is inconsistent with the general lack of faulting observed in the seismic sections. We are aware that there are alternative models. At the simplest level, our assumed initial crustal thickness of 43 km (equation (C4)) may be incorrect; in general, increasing crustal thickness increases synrift and total subsidence for a given β. However, we suggest that this uncertainty is less important than it appears for two reasons. First, it has no effect on the time constant of postrift subsidence, which depends on the total thickness of the lithosphere. Second, isostasy precludes a free choice in initial parameters. An increase in crustal thickness requires an increased crustal density or reduced mantle depletion, which diminishes the expected increase in subsidence. At a deeper level, we are aware that the constant temperature basal boundary condition of our model may be too simple. *Sleep* [2009] has applied a more sophisticated model using a parameterization of stagnant lid convection to the Michigan Basin. His model predicts an excess of synrift subsidence compared to the plate model, and there is indeed some evidence for this discrepancy in Figure 8. However, it requires an initial ponding of plume material at the time of extension, and there is no evidence in the Congo Basin for excessive volcanism and uplift at the time of rifting (early rocks indicate a shallow water environment that rapidly deepened). In any case, this modification does not alter the time constant of postrift subsi-

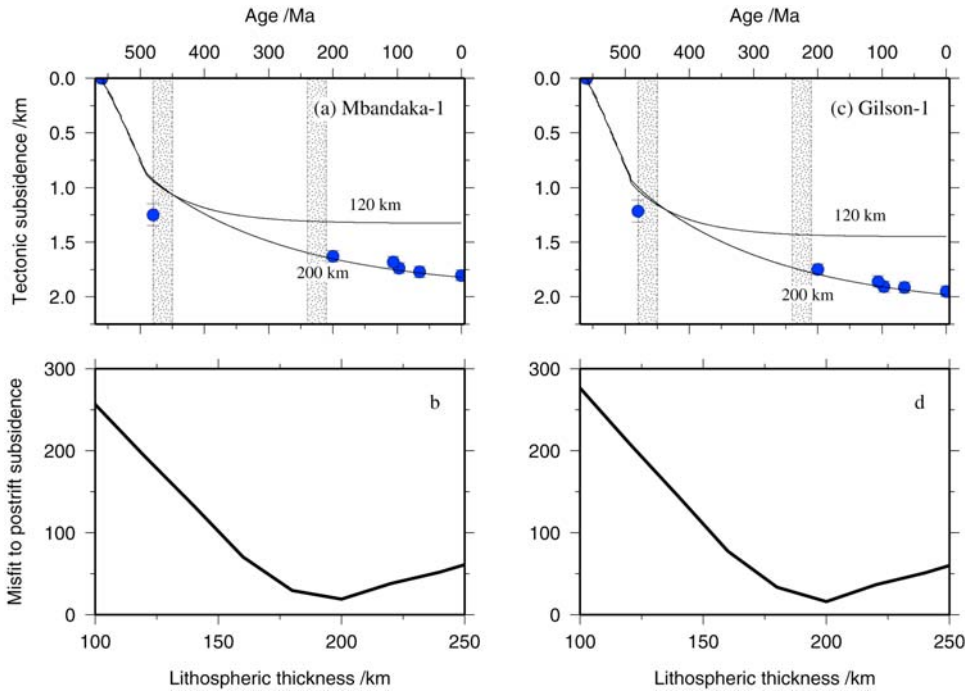

Figure 8. (a) Tectonic subsidence of Mbandaka-1 well calculated using the method of *Sclater and Christie* [1980]. Solid lines are predictions of the stretching model in Appendix C with lithosphere thicknesses of 120 and 200 km and a β of 1.2. Stippled bars show (mild) regional episodes of shortening. Subsidence can be accounted for by Cambrian extension of a thick lithospheric template by a factor of ~1.2 but not by extension of a normal template. The synrift subsidence is slightly greater than predicted because of possible lost section and selective drilling in deepest part of fault blocks (Figure 5). (b) Misfit function to the postrift horizons: the end of extension was fixed at 490 Ma (top Cambrian), and β was fixed to be 1.2 (Gilson) and 1.185 (Mbandaka). A similar pattern is found if β is also allowed to vary. Optimum fit is found when lithospheric thickness is ~200 km, which agrees with kimberlite geochemistry and surface wave tomography. (c and d) Tectonic subsidence and misfit of Gilson-1 well.

dence, and hence our argument about the role of thick lithosphere on basin subsidence.

[20] Finally, we observe that there is little sign of any sudden increase in accommodation space corresponding to an onset of mantle convective drawdown in Cenozoic times: clearly its effects are small and within the topographic depression. Examination of the interpreted cross sections in Figure 5 bears these trends out: there is local variation in the thickness of Cambrian sedimentary rocks (Lower Zaire sequence) as a result of the fault block geometry, but the thickness of the later Paleozoic (Upper Zaire sequence) and Mesozoic sediments is uniform across the basin and is unaffected by faulting, apart from some erosional truncation near prominent basement highs.

5. Gravity Modeling

[21] We now move from the history of the basin to discuss an important aspect of its present-day structure, which is the large negative long-wavelength gravity anomaly. There are two possible explanations. The first is that it is a static feature reflecting locally thickened lithosphere. The second is that it occurs because of convective downwelling beneath the lithospheric plate. We now explore each of these possibilities.

5.1. Option 1: Static Thick Lithosphere

[22] The first possibility is that the long-wavelength gravity anomaly results from lithosphere that is more dense than the reference column. If the lithosphere under the Congo Basin is thick, which Figures 2 and 6 and the work of *Batumike et al.* [2009] suggest it is, then a thermal density contrast does indeed exist, which in isolation will give rise to a gravity anomaly. In this model, the anomaly is negative because the signal is dominated by the shallower low-density crust and sediments, which are thicker than their surroundings in order to maintain isostatic equilibrium. The counter-

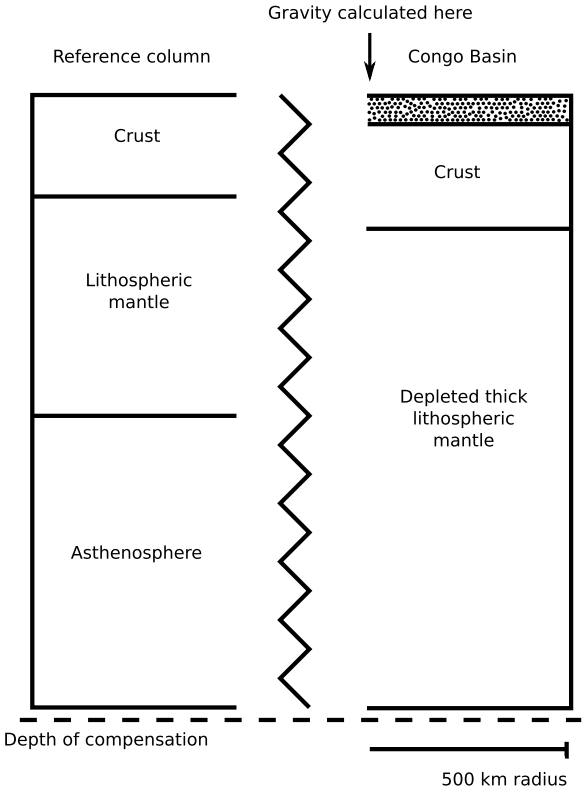

Figure 9. Cartoon illustrating the geometry of the gravity calculation to assess the gravitational expression of a region of thick lithosphere (Appendix B). Mantle density depletion is calculated to maintain isostatic equilibrium with the reference column. This corrected density distribution is then used to calculate the gravity anomaly at the center of the basin using equation (B1).

balancing lithospheric keel, which is more dense, has a smaller contribution because it is further away from the surface. However, this thick lithospheric keel is also less dense at standard conditions than the surrounding thin lithosphere because of chemical depletion (Appendix A). We therefore wish to know whether we can explain the observed gravity anomaly and still maintain isostatic equilibrium.

[23] To calculate the gravity anomaly at the center of the basin, we have used the disc model shown in Figure 9 (see also Appendix B). We use the model to estimate the difference in surface gravity between a 500 km radius disc of 200 km thick lithosphere overlain by 4 km of sediments (i.e., a much simplified Congo Basin) and a reference column at sea level with a 35 km crust and 125 km lithosphere. Since the thickness and density of the crust underneath the basin are unknown, we vary these systematically in order to identify combinations which will give rise to the observed −40 mGal long-wavelength anomaly. A final constraint is that both columns must balance isostatically at the base of the model, which is ensured by adjusting the density depletion of the thickened lithospheric mantle beneath the basin.

[24] Figure 10a shows the mean mantle depletion required for the columns to balance as a function of basin crustal thickness and density. Note that the global average is approximately 33 ± 16 kg m^{-3} (Figure A2). The corresponding gravity anomaly at the center of the disc as a function of basin crustal thickness and density is shown in Figure 10b, with the observed long-wavelength value (approximately −40 mGal) marked as a thick black line.

[25] The global trends summarized by equations (C4) and (C5) suggest that unstretched crust over 200 km lithosphere should have a mean density of approximately 2825–2875 kg m^{-3} and a thickness of approximately 40–45 km, which will reduce to 33–38 km after extension by a factor of 1.2. However, Figure 10b shows that the only way to account for the observed gravity anomaly is if the crust under the basin is either unexpectedly low in density, or unexpectedly thick. Moreover, all of these combinations imply a lithosphere that has negligible or negative depletion, which is in contrast to the trend in Figures A1 and A2, and to observations from kimberlite nodules. A crustal thickness of ~33 km and a density of 2875 kg m^{-3} require an expected mean depletion of ~33 kg m^{-3}, but produce a gravity anomaly at the center of the disc of only −10 mGal, which is a quarter of the observed value. We therefore argue that the gravity anomaly has an origin below the base of the lithosphere. If, on the other hand, its origin is in the lithosphere, both the crust and lithosphere under the basin must be anomalous compared to most other areas of thick lithosphere around the world (Figure A2). These conclusions are insensitive to the exact choice of reference column in Figure 9. This argument is essentially the conclusion reached by *Downey and Gurnis* [2009], who suggest that the anomalous mass is made of eclogite.

5.2. Option 2: Dynamic Topography

[26] In the second hypothesis, the gravity anomaly is generated by convective drawdown (i.e., anomalous dense mantle below the lithospheric lid). We investigate this possibility using a simple isostatic calculation.

[27] Above a region of buoyant anomalous mantle, *Crosby and McKenzie* [2009] showed that the

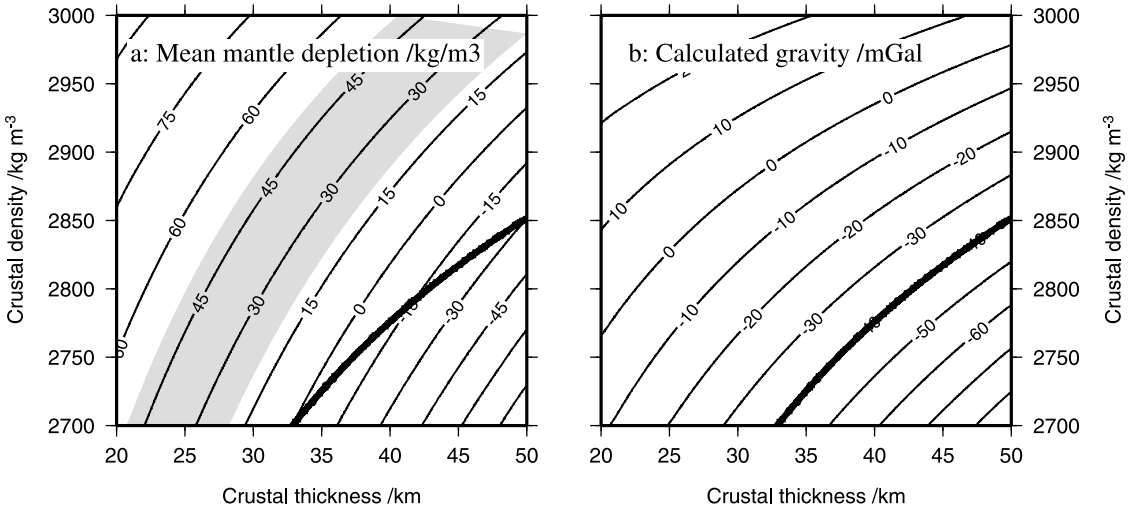

Figure 10. (a) Mean mantle depletion under the basin required by the geometry in Figure 9 to maintain isostatic equilibrium with the reference column, as a function of basement crustal thickness and density. The global average value for thick lithosphere is 20–50 kg m^{-3} (Figure 3) and is shown as a gray band. (b) Corresponding gravity anomalies at the center of the disc. The approximate mean value for the real basin (−40 mGal) is shown as a thick contour in both Figures 10a and 10b. Note that this value corresponds to negligible depletion in Figure 10a, which is inconsistent with Figures A1 and A2 and unrealistic. Furthermore, a basement crust of thickness 35 km corresponds to a mean density of 2800 kg m^{-3}, which is ~50 kg m^{-3} lighter than the global trend (equation (C5)).

isostatic admittance, Z, between topography and gravity is

$$Z \sim 2\pi G\rho_m\left(1 - e^{-2\pi d/\lambda}\right) \quad (1)$$

where d is the midpoint depth of the compensating mass in the mantle and λ is its lateral (full) wavelength. For the Congo Basin, λ is in the range 2000–2500 km and d is probably in the range 200–300 km since the lithosphere is at least twice as thick as old ocean. If the surface topography is dynamically supported, equation (1) implies that Z should be in the range 55–75 mGal/km, which is similar to that observed at wavelengths longer than 500 km [*Crosby*, 2006]. A −40 mGal gravity anomaly therefore requires a surface depression of 0.5–0.7 km, which implies that in the absence of convective drawdown the basin would be at an elevation of ~600 m. In other words we predict that it would form part of the African Superswell [*Nyblade and Robinson*, 1994], which is not associated with a significant gravity anomaly. In this simple model, the sediment fill itself is supported isostatically by changes in crustal thickness and mostly predates the drawdown.

[28] In terms of supporting evidence, global shear velocity model S20RTS shows that the Congo Basin is underlain by anomalously fast velocities to the base of the upper mantle which, in section, look remarkably like a convective drawdown [*Ritsema et al.*, 1999] (Figure 11). A recent tomography-based model of mantle convection by *Forte et al.* [2010] also predicts a strong downwelling under the Congo Basin driven by surrounding upwellings [e.g., *Al Hajri et al.*, 2009]. This argument requires that present-day drawdown and larger-scale regional uplift were not synchronous. It is possible that part of the dynamically supported load is sediment rather than air, in which case a smaller anomalous elevation is required. However, if the Mesozoic growth of sediment-filled accommodation space is due to drawdown, as *Hartley and Allen* [1994] suggested, then the subsidence modeling requires a thinner lithospheric template, which is inconsistent with the seismic velocity structure and kimberlite geochemistry at the present day (Figure 6) [*Batumike et al.*, 2009].

6. Discussion and Conclusions

[29] The existence of the Congo basin poses two important questions. The first is whether the growth of accommodation space is the product of lithospheric extension or whether there is a different mechanism. The second is the cause of the gravity anomaly. We believe that these two questions are related, and their answers have important implications for other intracratonic basins.

[30] Lower Cambrian normal faults which can be inferred in seismic reflection sections such as those

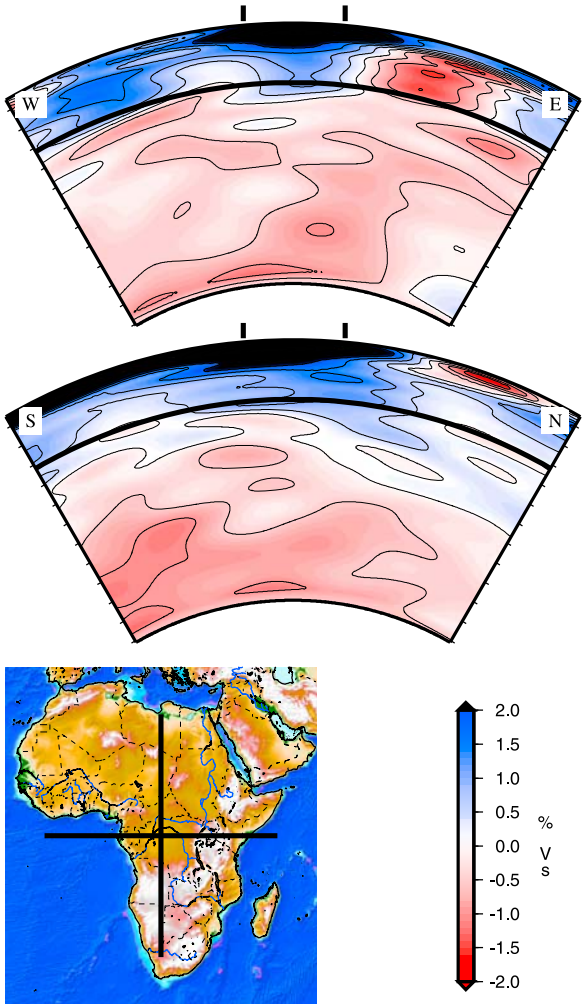

Figure 11. North-south and east-west sections from global shear wave velocity model S20RTS [*Ritsema et al.*, 1999]. Congo Basin is delineated by thick vertical lines. Note apparent downwelling under the thick lithospheric keel and the large lower mantle anomaly which coincides with the Southern African Superswell.

shown in Figure 4 provide clear evidence for crustal extension at the time the earliest sediments were deposited, and the continued growth of unfaulted accommodation space (albeit with hiatuses) for subsequent cooling of the extended mantle lithosphere. Estimates of the extension factors from subsidence modeling and the summation of horizontal fault displacements are consistent. There can therefore be little doubt that the basin is at least partly extensional in nature. The origin of this extension is unclear, especially why it should coincide with thick, rather than thin, lithosphere; we simply note that extension was widespread globally with the breakup of the supercontinent Rodinia in latest Proterozoic times [e.g., *Klein and Hsui*, 1987; *Torsvik et al.*, 1996]. The question is then whether cooling of stretched mantle lithosphere can account for the long (500–600 Ma) history of the basin. The surface wave tomography illustrated in Figure 6 and the kimberlite geochemical measurements of *Batumike et al.* [2009] suggests that it can: the lithosphere at the present day is substantially thicker than normal (~200 km rather than ~120 km), which suggests that at least this thickness existed at the time of extension. Since the thermal time constant of the lithosphere varies as the square of its thickness, Figure 8 then shows how the long history of the basin is consistent with lithospheric cooling after extension. The large (~100 km) size of the horst blocks is also consistent with a template that is thicker and cooler than normal. Although the basin has undoubtedly experienced more than one phase of shortening [e.g., *Daly et al.*, 1991, 1992], the subsidence curves in Figure 8 suggest that the shortening factor is considerably smaller than the initial extension factor, and that its effect on lithospheric geotherms has been minor.

[31] However, this conclusion presents a dilemma for explaining the origin of the gravity anomaly. If it is due to convective drawdown in the asthenosphere, as a number of authors have suggested, then this accommodation space must be filled by air, since extra accommodation space is not required according to the sedimentary subsidence record. Furthermore, the basin before drawdown must have been at an elevation of approximately 600 m. However, it is not clear if the African Superswell extends this far north, or whether all the eroded sediment since the onset of surrounding uplift would have accumulated offshore in the large Congo delta rather than in the continental basin. The alternative hypothesis, that the gravity anomaly is due solely to the thick lithosphere, is easier to reconcile with the subsidence record and the map of lithospheric thickness in Figure 6b, but not with the trend illustrated in Figures A1 and A2, which is that thick lithosphere is chemically depleted. It is also likely that the undepleted, dense, and therefore unusual, lithosphere required to match the gravity would have been gravitationally unstable, and would not have survived for the duration of the basin's history. These results are also inconsistent with global tomographic model S20RTS (Figure 11) [*Ritsema et al.*, 1999] which shows clearly a drawdown-like region of fast velocities underneath the lithosphere below the basin; and the models of *Forte et al.* [2010], who calculate mantle flow patterns using seismic tomographic models TX2007 and TX2008 [*Simmons et al.*, 2009], esti-

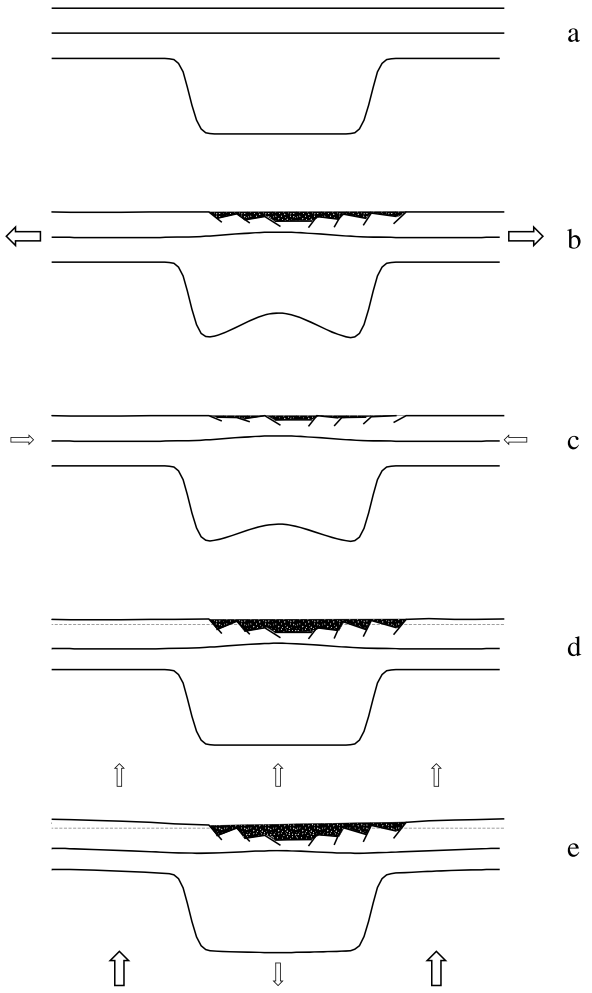

Figure 12. Cartoon showing proposed evolution of the intracratonic Congo Basin. (a) Initial template prior to ~600 Ma. Boundaries are surface, Moho, and base of lithosphere. (b) Latest Precambrian extension by a factor of approximately 1.2 thins crust and mantle lithosphere and generates normal faulting. (c) Minor Cambro-Ordovician (Pan-African) shortening and erosive loss of section. May have been repeated more than once. (d) Regional Cenozoic uplift corresponding to Southern African Superplume. Dashed line denotes sea level. Basin is now almost thermally mature and is only growing slowly. (e) Present-day modulation by upper mantle convection raises flanks and depresses interior to near sea level. Magnitude of interior depression is smaller than flank uplift, but areal extent is greater. Diagrams not to scale.

mates of $\partial\rho/\partial V_s$ and mantle viscosity, and predict a clear and substantial downwelling underneath the basin. We note, however, that not all tomographic models are in agreement with this interpretation [e.g., *Kustowski et al.*, 2008].

[32] We suggest that the most likely explanation is a combination, which is that a depleted, but not isopycnal, lithospheric keel forces the cooling horizontal flow from adjacent upwelling plumes downward (see Figure 1). We note this is the same conclusion as reached by *Forte et al.* [2010]. This flow may be as young as Neogene in age given the recent uplift of the adjacent coastline [*Al Hajri et al.*, 2009]. A summary cartoon is given in Figure 12. Figure 10 shows that even a lithospheric keel with a mean depletion of 20–30 kg m^{-3} (the global average, Figure A1) will result in a gravity anomaly of approximately −10 mGal, implying that only −30 mGal is attributable to drawdown, corresponding to an air load (and thus pre-Neogene elevation) of ~400 m. Drawdown is also consistent with the compressional earthquake focal mechanisms observed within the basin (Figure 2d).

[33] It is important to state again at this stage that we agree with *Daly et al.* [1991, 1992] that the basin contains complex features reflecting several distinct tectonic episodes, which is unsurprising for a region the size of western Europe that has been in existence for more than half a billion years. Growth of the sedimentary section has not been continuous and there has clearly been both uplift and erosion, some of which was due to mild tectonic shortening, and some of which was likely due to mantle convection (as is the case today). However, these details do not negate the most important unexplained question, which is why the basin has kept growing for such a long period of geological time. Horizontal deformation of the crust and mantle lithosphere since initial rifting is not the answer: the stratigraphic extent of normal faulting implies that there has been no significant extension since the end of Cambrian time, and, away from flexural foreland basins, which are not in evidence here, shortening causes uplift, not subsidence. Mantle convection best explains the present-day gravity field but has little obvious expression in the backstripped subsidence record, and is we argue only part of the answer. By contrast, we assert that the thermal subsidence of thick lithosphere in response to mild extension in latest Precambrian and early Cambrian time, followed by recent two-stage surface modulation by mantle dynamic processes, does provide a simple explanation for the evolution of the Congo Basin at the largest scale, and is the framework against which the many, and undoubted, smaller-scale geological complexities should be set.

[34] In terms of extending our understanding in the absence of future hydrocarbon exploration, the most important advance would be the installation of a broadband seismometer within the deep basin and calculation of receiver functions. We currently have no direct constraints on crustal thickness,

which are essential for constraining gravity models and extension factors. Moreover, if there is a large downwelling plume, as the gravity data (Figure 2c) and deep seismic tomography (Figure 11) suggest, the 410 km and 670 km mantle discontinuites should be deflected by a detectable amount.

[35] What are the implications for other intracratonic basins? Comparisons are not straightforward because very few other cratonic basins have the same combination of seismic reflection data, boreholes through the synrift and postrift sections, and a sedimentary record that spans at least two thermal time constants. The Michigan Basin is the classic intracratonic basin [e.g., *Sleep*, 2009, and references therein], but there is no available deep seismic reflection data and no section younger than 200 Ma. The Taoudeni Basin in Mauritania has accumulated sedimentary rocks from the Upper Proterozoic until Mesozoic time, is underlain by normal faults [*Villeneuve*, 2005], and coincides with both anomalously thick lithosphere and a 10–20 mGal negative gravity anomaly and is a possible analog, but published data is otherwise sparse. The Precaspian Basin in Kazakhstan also occurs within thick lithosphere, has an areal extent of similar size and shape to the Congo Basin, a 20–30 mGal regional negative gravity anomaly, and a similar time scale of sedimentary accumulation. However, there are no deep penetrations and the total thickness of sedimentary rocks is at least a factor of 3 larger than the Congo [*Brunet et al.*, 1999; *Volozh et al.*, 2003]. Finally, the Hudson Bay basin may also be an analog: although much of the sedimentary record has been lost because of erosion [*Hanne et al.*, 2004], it is underlain by normal faulting and coincides with both extremely thick lithosphere and a large ~30 mGal negative gravity anomaly, less than 45% of which can be explained by incomplete postglacial adjustment [*Tamisiea et al.*, 2007]. In each case, testing the extensional and drawdown hypotheses will require careful examination of the primary seismic reflection data, subsidence modeling and gravity modeling. Only then will we be able to understand if the Congo basin is unique, or whether it is an example of a more general class of extensional basins.

Appendix A: Steady State Density Profiles and Isostatic Depletion Analysis

[36] Steady state temperature profiles are calculated using the method given by *McKenzie et al.* [2005]. The structure of the thermal boundary layer is neglected, although we note that the convective process responsible for maintaining the temperature at the base of the plate becomes less vigorous with increasing lithospheric thickness as the required mantle heat flow decreases. In the mantle, density is related to temperature by a variable coefficient of thermal expansion [*Bouhifd et al.*, 1996].

$$\alpha = 2.832 \times 10^{-5} T + 0.758 \times 10^{-8} T^2 \qquad \text{(A1)}$$

The density at 0 K is taken to be 3360 kg m^{-3}. For the crust, α is taken to be 2.4 × 10^{-5} K^{-1}, and its density at 0 K is variable, as discussed in the text.

[37] In Figure A1 we use isostatic considerations to calculate the mean depletion of the lithospheric mantle globally with respect to the MORB source using seismic estimates of lithospheric thickness [*Priestley and McKenzie*, 2006; *McKenzie and Priestley*, 2008; this study]. If we first assume that lithospheric mantle is in steady state and that the only control on density is temperature, any discrepancy between the calculated masses of the continental and oceanic columns can be attributed to either chemical depletion or to thermal disequilibrium. Figure A1 shows that where the lithosphere is thin, the data show considerable scatter. We suspect that both thermal disequilibrium after past extension and errors in lithospheric thickness estimates are the dominant causes of this scatter. However, where the lithosphere is thick, the data cluster more tightly, and we suspect chemical depletion is the main cause. A histogram of depletion estimates is shown in Figure A2 together with the results of Monte Carlo error analysis, which shows that these results are robust.

[38] Our data have a number of different sources. The crustal thickness part of each continental column is extracted from our own comprehensive worldwide database of ~1900 receiver functions from the published literature, from which only those near sea level are used. Estimates of the mean crustal density at each location are taken from CRUST 2.0 which is based on a large synthesis of seismic refraction profiles and velocity-density functions [*Laske and Masters*, 1997]. Finally, the reference oceanic column is defined using knowledge of the depth and lithospheric thickness of mature ocean floor [*Crosby et al.*, 2006]. Figure A1 shows that our results are consistent with the kimberlite estimates: once lithosphere thicknesses exceed 150 km, mean density depletion within the lithosphere is 33 ± 16 kg m^{-3}. Monte Carlo error analysis in Figure A2 shows that these values are significant. They also agree within error to those

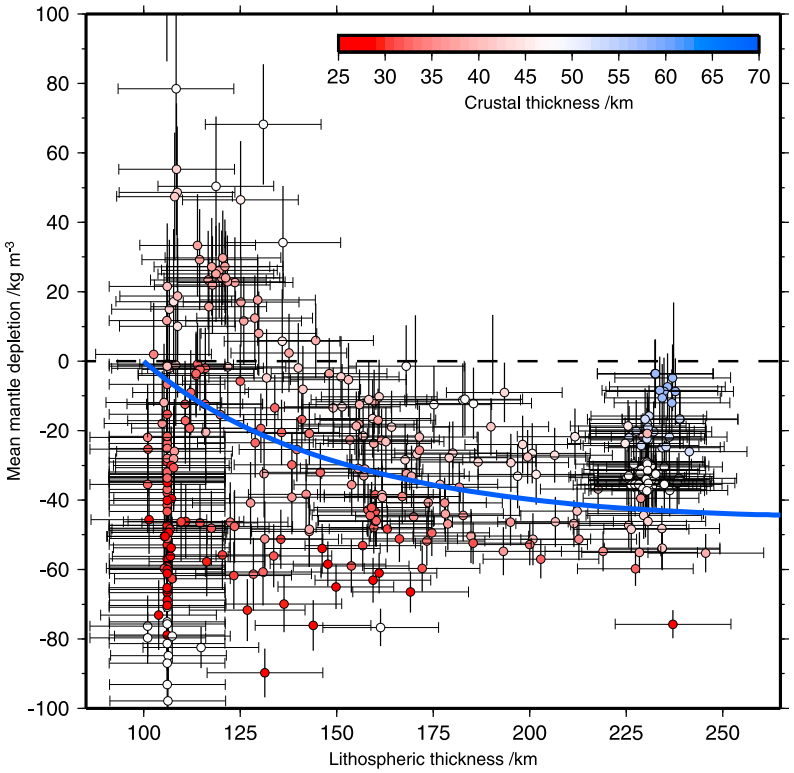

Figure A1. Estimates of mean mantle density depletion worldwide, found by calculating the excess column mass above that required for isostatic equilibrium with old ocean floor if temperature is the only control on mantle density. Crustal thickness estimates are from a database of ~1900 published receiver functions, using data only from regions assumed to be in thermal steady state. Mean crustal density estimates are from CRUST2.0 (G. Laske et al., CRUST 2.0: A new global crustal thickness model at 2 × 2 degrees, available at http://mahi.ucsd.edu/gabi/rem.html) [see also *Bassin et al.*, 2000], and lithosphere thickness estimates are from *Priestley and McKenzie* [2006] and this study. Once lithospheric thicknesses exceed 150 km, mean depletion is 30 ± 20 kg m^{-3}. Horizontal error bars are a fixed 15 km; vertical error bars are calculated by varying the mean crustal density by ±30 kg m^{-3}. Solid line shows the isopycnal condition.

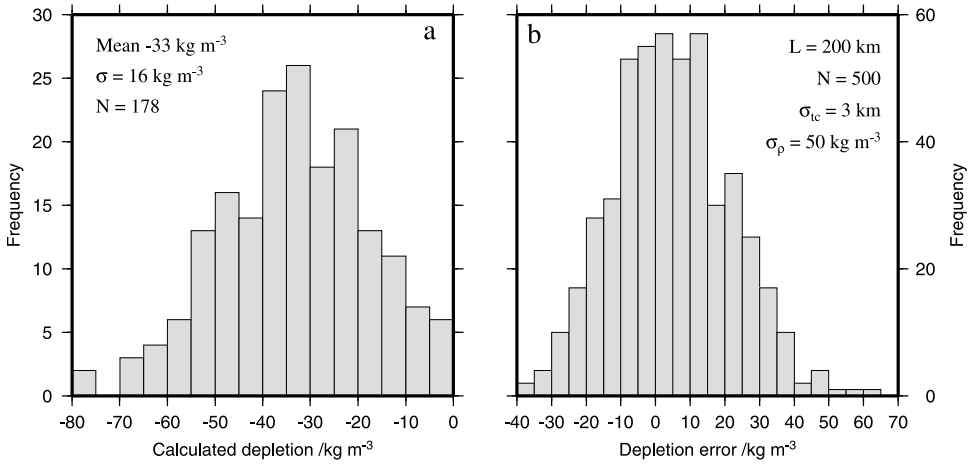

Figure A2. (a) Histogram of calculated mean mantle depletion when lithospheric thickness is greater than 150 km. Mean and standard deviation are 33 and 16 kg m^{-3}, respectively. (b) Effect of errors in crustal thickness and density on calculated depletion. The starting model has a lithospheric thickness of 200 km, a crustal thickness of 43 km, and mean density of 2877 kg m^{-3}, resulting in a calculated depletion of 20 kg m^{-3}. Five hundred random perturbations to this template have a Gaussian distribution with standard deviations of 3 km and 50 kg m^{-3}. The standard deviation of the calculated depletion estimates is 16 kg m^{-3}, which is the same as the real data in Figure A2a.

obtained in an earlier study by *Kaban et al.* [2003] based on gravity modeling, and on estimates mantle nodules and mineral physics [e.g., *Hawkesworth et al.*, 1990; *Schutt and Lesher*, 2006]. In conclusion, worldwide isostatic estimates of mean lithospheric mantle depletion are consistent with those from kimberlite nodules, but are not quite isopycnal. We note that this isostatic approach does not constrain the variation of depletion with depth. Using global tomographic models, *Forte and Perry* [2000] have argued that depletion reaches a peak at a depth of ~130 km and diminishes to negligible amplitudes at the base of the lithosphere.

[39] Density also varies laterally at a given temperature because of slight differences in gravitational self-compression. An upper limit to this variation may be approximated using a simple model of a radially symmetric Earth structure [e.g., *Fowler*, 2005], such that

$$\frac{d\rho}{dz} = \frac{GM_r\rho}{(R-z)^2\phi} - \alpha\rho\tau \tag{A2}$$

where G is the gravitational constant, M_r is the mass of the Earth enclosed within a sphere of radius smaller than z, R is the radius of the Earth, $\phi = v_p^2 - 4/3v_s^2$ is the seismic parameter and τ is the superadiabatic temperature gradient. Compositional boundaries such as the Moho alter the density in sudden steps and must be added manually to the integration. Including this correction increases our estimate of the mean density depletion of thick lithosphere from approximately 33 ± 16 kg m^{-3} (Figure A2) to 50 ± 20 kg m^{-3}. However, we still observe the same discrepancy in terms of the amount of depletion under the Congo basin required by the static gravity anomaly modeling compared to the global average (Figure 10).

Appendix B: Calculation of Gravity Anomalies at the Center of a Cylinder

[40] The gravity anomaly over the center of a disc with anomalous density $\Delta\rho(z)$, thickness h and radius R is [*Turcotte and Schubert*, 2002]

$$\Delta g = 2\pi G \int_0^h \Delta\rho(z)\left(1 - \frac{z}{\sqrt{R^2+z^2}}\right)dz \tag{B1}$$

where $\Delta\rho(z)$ is the lateral difference in density between the anomalous and reference lithospheric columns and is calculated as described in Appendix A. We follow *Kaban et al.* [2003] and use a simple model in which the adjustment is $2\Delta\overline{\rho_m}$ immediately under the Moho, zero at the base of the lithosphere, and decreases linearly in between, although we acknowledge that more complex models are possible [e.g., *Forte and Perry*, 2000; *Simmons et al.*, 2009].

Appendix C: A Modified 1-D Stretching Model for Thick Lithosphere

[41] To calculate the change in temperature structure with time (t) during and after uniform extension of the lithosphere,

$$\frac{\partial}{\partial t}(\rho c_p T) = \frac{\partial}{\partial z}\left(k\frac{\partial T}{\partial z}\right) + Gz\frac{\partial}{\partial z}(\rho c_p T) + H \tag{C1}$$

is solved numerically using a simple finite difference method with the steady state starting condition described in Appendix A. Because the basin is wide (~500 km radius), lateral conduction of heat can be neglected [e.g., *Kaminski and Jaupart*, 2000]. Crustal extension factor, β, is related to strain rate, G, by

$$\beta = \exp\left(\int_0^t G dt\right) \tag{C2}$$

and the total water-loaded subsidence is

$$s(t) = \frac{1}{\rho_a - \rho_w}\int_0^L [\rho(z,\infty) - \rho(z,t)]dz \tag{C3}$$

where ρ_a is the density of the asthenosphere and L is the thickness of the lithosphere. This calculation includes the advective thinning of the chemically depleted lithospheric root. The crustal thickness, t_c, and density, ρ_c, vary with lithosphere thickness in km as

$$t_c = 0.12L + 19 \text{ km} \tag{C4}$$

$$\rho_c = 2711 + 0.83L \text{ kg m}^{-3} \tag{C5}$$

which are the best fit linear trends to the data used to generate Figure A1.

[42] These data also explain why synrift subsidence occurs when thick lithosphere is stretched. A simple isostatic mass balance shows that synrift uplift (discussed by *McKenzie* [1978] as a possibility more likely with thick lithosphere) will only occur when the mean mantle density, $\overline{\rho_m}$, is greater than

$$\overline{\rho_m} = \frac{L\rho_a - t_c\rho_c}{L - t_c} \tag{C6}$$

or 3275 kg m^{-3} given a crustal density of 2875 kg m^{-3} and thickness of 43 km, which is ~50 kg m^{-3} too heavy to balance against a mid-ocean ridge.

Acknowledgments

[43] This research is funded by BP Exploration and forms a broader part of the BP-Cambridge Margins Research Program. We are grateful to K. Dawkes, J. Jackson, L. Mackay, D. McKenzie, K. Priestley, G. Roberts, E. Rogers, and H. Walford for helpful discussions. The data for the tomographic study were obtained through the IRIS Data Management Centre and include the GEOSCOPE, GEOFON, and GSN permanent stations and the PASSCAL and SEIS-UK temporary deployments. We thank G. Helffrich for generously providing seismic data from the Cape Verde Islands. T. Becker, A. Forte, N. Sleep, and an anonymous reviewer provided a number of useful suggestions for improving the manuscript. This study is Earth Sciences contribution 1396.

References

Al Hajri, Y., N. White, and S. Fishwick (2009), Scales of transient convective support beneath Africa, *Geology*, *37*, 883–886.

Armitage, J. J., and P. A. Allen (2010), Cratonic basins and the long-term subsidence history of continental interiors, *J. Geol. Soc.*, *167*, 61–70.

Ayele, A. (2002), Active compressional tectonics in central Africa and implications for plate tectonic models: Evidence from fault mechanism studies of the 1998 earthquakes in the Congo Basin, *J. Afr. Earth. Sci.*, *35*, 45–50.

Bassin, C., G. Laske, and G. Masters (2000), The current limits of resolution for surface wave tomography in North America, *Eos Trans. AGU*, *81*(48), Fall Meet. Suppl., Abstract S12A-03.

Batumike, J. M., W. L. Griffin, and S. Y. O'Reilly (2009), Lithospheric mantle structure and diamond potential of kimberlites in southern D. R. Congo, *Lithos*, *112*, 166–176.

Begg, G. C., et al. (2009), The lithospheric architecture of Africa: Seismic tomography, mantle petrology, and tectonic evolution, *Geosphere*, *5*, 23–50.

Bouhifd, M. A., D. Adrault, G. Fiquet, and P. Richet (1996), Thermal expansion of forsterite up to the melting point, *Geophys. Res. Lett.*, *10*, 285–301.

Brunet, M.-F., Y. A. Volozh, M. P. Antipov, and L. I. Lobkovsky (1999), The geodynamic evolution of the Precaspian Basin (Kazakhstan) along a north-south section, *Tectonophysics*, *313*, 85–106.

Crosby, A. G. (2006), Aspects of the relationship between topography and gravity on the Earth and Moon, Ph.D. thesis, Univ. of Cambridge, Cambridge, U. K.

Crosby, A. G., and D. McKenzie (2009), An analysis of young ocean depth, gravity and global residual topography, *Geophys. J. Int.*, *178*, 1198–1219.

Crosby, A. G., D. McKenzie, and J. G. Sclater (2006), The relationship between depth, age and gravity in the oceans, *Geophys. J. Int.*, *166*, 553–573.

Daly, M. C., S. R. Lawrence, D. Kimuna'a and M. Binga (1991), Late Paleozoic deformation in Central Africa: A result of distant collision?, *Nature*, *350*, 605–607.

Daly, M. C., S. R. Lawrence, K. Diemu-Tshiband, and B. Matouana (1992), Tectonic evolution of the Cuvette Centrale, Zaire, *J. Geol. Soc. London*, *149*, 539–546.

Debayle, E. (1999), Sv-wave azimuthal anisotropy in the Australian upper mantle: Preliminary results from an automated Rayleigh waveform inversion, *Geophys. J. Int.*, *137*, 747–754.

Downey, N. J., and M. Gurnis (2009), Instantaneous dynamics of the cratonic Congo basin, *J. Geophys. Res.*, *114*, B06401, doi:10.1029/2008JB006066.

Exploration Consultants Ltd. (ECL) (1988), The hydrocarbon potential of Cuvette Centrale (Republic of Zaire), industrial report, CTP Petrozaire, Houston, Tex.

Fishwick, S., and A. M. Reading (2008), Anomalous lithosphere beneath the Proterozoic of western and central Australia: A record of continental collision and intraplate deformation, *Precambrian Res.*, *166*, 111–121.

Fishwick, S., B. L. N. Kennett, and A. M. Reading (2005), Contrasts in lithospheric structure within the Australian Craton—Insights from surface wave tomography, *Earth Planet. Sci. Lett.*, *231*, 163–176.

Forte, A. M., and H. K. C. Perry (2000), Geodynamic evidence for a chemically depleted continental tectosphere, *Science*, *290*, 1940–1944.

Forte, A. M., et al. (2010), Joint seismic-geodynamic-mineral physical modelling of African geodynamics: A reconciliation of deep-mantle convection with surface geophysical constraints, *Earth Planet. Sci. Lett.*, doi:10.1016/j.epsl.2010.03.017, in press.

Foster, A. N., and J. Jackson (1998), Source parameters of large African earthquakes: Implications for crustal rheology and regional kinematics, *Geophys. J. Int.*, *134*, 422–448.

Foster, A., and F. Nimmo (1996), Comparisons between the rift systems of East Africa and Beta Regio, Venus, *Earth Planet. Sci. Lett.*, *143*, 183–195.

Fowler, C. M. R. (2005), *The Solid Earth: An Introduction to Global Geophyics*, 2nd ed., Cambridge Univ. Press, Cambridge, U. K.

Giresse, P. (2005), Mesozoic-Cenozoic history of the Congo Basin, *J. Afr. Earth. Sci.*, *43*, 301–315.

Godey, S., F. Deschamps, J. Trampert, and R. Snieder (2004), Thermal and compositional anomalies beneath the North American continent, *J. Geophys. Res.*, *109*, B01308, doi:10.1029/2002JB002263.

Goes, S., R. Govers, and P. Vacher (2000), Shallow mantle temperatures under Europe from P and S wave tomography, *J. Geophys. Res.*, *105*, 11,153–11,169.

Grand, S. P. (2002), Mantle shear wave tomography and the fate of subducted slabs, *Philos. Trans. R. Soc. London, Ser. A*, *360*, 2475–2491.

Hanne, D., N. White, A. Butler, and S. Jones (2004), Phanerozoic vertical motions of Hudson Bay, *Can. J. Earth. Sci.*, *41*, 1181–1200.

Hartley, R., and P. A. Allen (1994), Interior cratonic basins of Africa: Relation to continental break-up and role of mantle convection, *Basin Res.*, *6*, 95–113.

Hawkesworth, C. J., P. D. Kempton, N. W. Rogers, R. M. Ellam, and P. W. Calsteren (1990), Continental mantle lithosphere, and shallow level enrichment processes in the Earth's mantle, *Earth Planet. Sci. Lett.*, *96*, 256–268.

Huerta, A. D., A. A. Nyblade, and A. M. Reusch (2009), Mantle transition zone beneath Kenya and Tanzania: More evidence for a deep-seated thermal upwelling in the mantle, *Geophys. J. Int.*, *177*, 1249–1255.

Jordan, T. H. (1978), Composition and development of the continental tectosphere, *Nature*, *274*, 544–548.
Kaban, M. K., P. Schwintzer, I. M. Artemieva, and W. D. Mooney (2003), Density of continental roots: Compositional and thermal contributions, *Earth Planet. Sci. Lett.*, *209*, 53–69.
Kaminski, E., and C. Jaupart (2000), Lithosphere structure beneath Phanerozoic intracratonic basins of North America, *Earth Planet. Sci. Lett.*, *178*, 139–149.
Klein, G. d., and A. T. Hsui (1987), Origin of cratonic basins, *Geology*, *15*, 1094–1098.
Kominz, M. A., D. Werkema, D. A. Barnes, W. Harrison, E. Kirwan, and M. Malin (2001), The Michigan Basin is thermal in origin, *AAPG Bull.*, *85*, 1533–1534.
Kustowski, B., G. Ekström, and A. M. Dziewonski (2008), Anisotropic shear-wave velocity structure of the Earth's mantle: A global model, *J. Geophys. Res.*, *113*, B06306, doi:10.1029/2007JB005169.
Laske, G., and T. G. Masters (1997), A global digital map of sediment thickness, *EOS Trans. AGU*, *78*(46), Fall Meet. Suppl., F483.
Lawrence, S. R., and M. M. Makazu (1988), Zaire's Central Basin: Prospectivity outlook, *Oil Gas J.*, *86*, 105–108.
Lebedev, S., J. Boonen, and J. Trampert (2009), Seismic structure of Precambrian lithosphere: New constraints from broadband surface wave dispersion, *Lithos*, *109*, 96–111.
McKenzie, D. (1978), Some remarks on the development of sedimentary basins, *Earth Planet. Sci. Lett.*, *40*, 25–32.
McKenzie, D., and D. Fairhead (1997), Estimates of the effective elastic thickness of the continental lithosphere from Bouguer and free-air gravity anomalies, *J. Geophys. Res.*, *102*, 27,523–27,552.
McKenzie, D., and K. Priestley (2008), The influence of lithospheric thickness variations on continental evolution, *Lithos*, *102*, 1–11.
McKenzie, D., J. Jackson, and K. Priestley (2005), The thermal structure of oceanic and continental lithosphere, *Earth Planet. Sci. Lett.*, *233*, 337–349.
Newman, R., and N. White (1999), The dynamics of extensional sedimentary basins: Constraints from subsidence inversions, *Philos. Trans. R. Soc. London*, *357*, 805–834.
Nyblade, A. A., and S. W. Robinson (1994), The African Superswell, *Geophys. Res. Lett.*, *21*, 765–768.
Pasyanos, M., and A. A. Nyblade (2007), A top to bottom lithospheric study of Africa and Arabia, *Tectonophysics*, *444*, 27–44.
Pedersen, H. A., S. Fishwick, and D. B. Snyder (2009), A comparison of cratonic roots through consistent analysis of seismic surface waves, *Lithos*, *109*, 81–95.
Peltier, W. R., A. M. Forte, J. X. Mitrovica, and A. M. Dziewonski (1992), Earth's gravitational field: Seismic tomography resolves the enigma of the Laurentian anomaly, *Geophys. Res. Lett.*, *19*, 1555–1558.
Perry, H. K. C., A. M. Forte, and D. W. S. Eaton (2003), Upper mantle thermochemical structure below North America from seismic-geodynamic flow models, *Geophys. J. Int.*, *154*, 279–299.
Priestley, K., and D. McKenzie (2006), The thermal structure of the lithosphere from shear wave velocities, *Earth Planet. Sci. Lett.*, *244*, 285–301.
Ritsema, J., and H. van Heijst (2000), New seismic model of the upper mantle beneath Africa, *Geology*, *28*, 63–66.
Ritsema, J., H. van Heijst, and J. H. Woodhouse (1999), Complex shear wave velocity structure imaged beneath Africa and Iceland, *Science*, *286*, 1925–1928.
Sclater, J. G., and P. A. F. Christie (1980), Continental stretching: An explanation of the post-Mid Cretaceous subsidence of the Central North Sea Basin, *J. Geophys. Res.*, *85*, 3711–3739.
Schutt, D. L., and C. E. Lesher (2006), Effects of melt depletion on the density and seismic velocity of garnet and spinel lherzolite, *J. Geophys. Res.*, *111*, B05401, doi:10.1029/2003JB002950.
Sebai, A., E. Stutzmann, J. P. Montagner, D. Sicilia, and E. Beucler (2006), Anisotropic structure of the African upper mantle from Rayleigh and Love wave tomography, *Phys. Earth Planet. Inter.*, *155*, 48–62.
Simmons, N., A. M. Forte, and S. P. Grand (2009), Joint seismic, geodynamic and mineral physical constraints on three-dimensional mantle heterogeneity: Implications for the relative importance of thermal versus compositional heterogeneity, *Geophys. J. Int.*, *177*, 1284–1304.
Sleep, N. H. (2009), Stagnant lid convection and the thermal subsidence of sedimentary basins with reference to Michigan, *Geochem. Geophys. Geosyst.*, *10*, Q12015, doi:10.1029/2009GC002881.
Sleep, N. H., and L. L. Sloss (1978), A deep borehole in the Michigan Basin, *J. Geophys. Res.*, *83*, 5815–5819.
Tainton, K. M., and D. McKenzie (1994), The generation of kimberlites, lamproites and their source rocks, *J. Petrology*, *35*, 787–817.
Tamisiea, K. M., J. X. Mitrovica, and J. L. Davis (2007), GRACE gravity data constrain ancient ice geometries and continental dynamics over Laurentia, *Science*, *316*, 881–883.
Tapley, B. J., et al. (2005), GGM02—An improved Earth gravity field model from GRACE, *J. Geod.*, *79*, 467–478, doi:10.1007/s00190-005-0480-z.
Tibi, R., A. M. Larson, A. A. Nyblade, P. J. Shore, P. A. Wiens, J. M. Nnange, C. Taboud, and A. Bekoc (2005), A broadband seismological investigation of the Cameroon Volcanic Line, *Eos Trans. AGU*, *86*(52), Fall Meet. Suppl., Abstract S11B-0170.
Torsvik, T. H., M. A. Smethurst, J. G. Meert, R. Van der Voo, W. S. McKerrow, M. D. Brasier, B. A. Sturt, and H. J. Walderhaug (1996), Continental break-up and collision in the Neoproterozoic and Paleozoic—A tale of Baltica and Laurentia, *Earth Sci. Rev.*, *40*, 229–258.
Turcotte, D. L., and G. Schubert (2002), *Geodynamics*, 2nd ed., Cambridge Univ. Press, Cambridge, U. K.
Villeneuve, M. (2005), Paleozoic basins in West Africa and the Mauritanide thrust belt, *J. Afr. Earth. Sci.*, *43*, 166–195.
Volozh, Y. A., M. P. Antipov, M.-F. Brunet, I. A. Garagash, L. I. Lobkovsky, and J.-P. Cadet (2003), Pre-Mesozoic geodynamics of the Precaspian Basin (Kazakhstan), *Sediment. Geol.*, *156*, 35–58.
Walford, H. L., and N. J. White (2005), Constraining uplift and denudation of the West African continental margin by inversion of stacking velocity data, *J. Geophys. Res.*, *110*, B04403, doi:10.1029/2003JB002893.
Walsh, J., J. Watterson, and G. Yielding (1991), The importance of small-scale faulting in regional extension, *Nature*, *351*, 391–393.
Weeraratne, D. S., D. W. Forsyth, K. M. Fischer, and A. A. Nyblade (2003), Evidence for an upper mantle plume beneath the Tanzanian craton from Rayleigh wave tomography, *J. Geophys. Res.*, *108*(B9), 2427, doi:10.1029/2002JB002273.
White, N. (1994), An inverse method for determining lithospheric strain rate variation on geological timescales, *Earth Planet. Sci. Lett.*, *122*, 351–371.